TREATMENT OF MURINE CUTANEOUS MELANOMA WITH NEAR INFRARED LIGHT

C. Dees[1], J. Harkins[1], M.G. Petersen[2], W.G. Fisher[1], and E.A. Wachter[*1]

[1]Photogen, Inc., Knoxville, TN, USA

[2]The University of Tennessee College of Veterinary Medicine, Knoxville, TN, USA

[*]To whom correspondence should be addressed at: Photogen, Inc., 7327 Oak Ridge Highway, Knoxville, TN 37931, USA. Phone: 865-69-4011; fax: 865-769-4013; e-mail: wachter@photogen.com

Abbreviations: H&E, hematoxylin and eosin; IFN-ã, interferon-ã; IL-2, interleukin-2; IL-10, interlukin-10; NIR, near infrared; PDT, photodynamic therapy.

ABSTRACT

Treatment of cutaneous melanoma (M-3 and B16-F10 implanted in mice) with rapidly-scanned, tightly-focused near infrared light elicits selective destruction of tumor tissue. A single laser treatment yielded >90% eradication of B16-F10 tumors with thicknesses exceeding 3 mm; amelanotic M-3 tumors proved less responsive (ca. 25% clearance rate). In addition to local tumor destruction, laser treatment stimulated enhanced cytokine levels (IL-2 and IL-10) within treated tumor tissues and rejection of tumor cells upon subsequent challenge dose. Such anti-tumor immune response may lead to improved outcome at both the treatment site and at sites of distant metastasis.

INTRODUCTION

Melanoma will afflict about 51,400 persons in the U.S. in 2001, with an incidence rate that is increasing about 3% per annum (1). While the disease is considered to be highly treatable upon early diagnosis, the prognosis upon onset of metastasis is dire, typified by a 13% five-year survival rate once distant malignancy has occurred. Aside from excision of the primary tumor, radiation therapy, chemotherapy, and immunotherapy are commonly used in an effort to control metastasis.

Photodynamic therapy (PDT) has proven successful for treatment of some forms of cancer (2), but delivering the necessary ultraviolet or visible activating light through highly pigmented melanoma tumor tissue has proven difficult (3), precluding effective photodynamic destruction of the entire tumor. While many of the biological precursors to melanin produce a potent cytotoxic response when exposed to UV light (4-6), and thus might be useful as endogenous photosensitizers, the absorbance of melanin normally precludes significant UV photoactivation within tumor tissue.

Non-linear activation (7) of synthetic melanin precursors has been demonstrated in vitro using near infrared (NIR) light from the titanium:sapphire laser (8), producing a multiphoton-excited state equivalent to that occurring upon absorption of a UV photon. Such light should be capable of penetrating several millimeters into tumor tissue (9), especially at wavelengths beyond 1000 nm, and might enable photodynamic treatment of tumors using eumelanin and pheomelanin precursors as naturally occurring photosensitizers. Linear absorption of such applied NIR light may also contribute to heating of melanin, and such heating could play an important role in therapeutic response (10, 11). Finally, recent revival of interest in possible anti-tumor immunologic response upon PDT (12-17) suggests that treatment of melanoma with NIR light might yield a useful immune response by unmasking antigenic materials sequestered within tumor tissues.

Thus, this work examines the role of non-linear and linear (i.e., hyperthermic) mechanisms in treatment of implanted murine melanomas, with additional assessment of immunologic response upon eradication of primary tumors.

MATERIALS AND METHODS

Animals and animal husbandry. Animal housing and care were based on standards established by the Association for Assessment and Accreditation of Laboratory Animal Care, International (AAALAC) and guidelines set forth in the Guide for the Care and Use of Laboratory Animals, NIH Publication No. 96-03, 1996.

Tumor models. B16-F10 melanoma tumors were implanted subcutaneously in one flank of 5-week old female mice (either C57BL/6 mice, Charles River Laboratories, Wilmington, MA, USA, or albino HSD: athymic nude-nu mice, Harlan Sprague Dawley, Indianapolis, IN, USA) by injection of approximately 10^6 B16-F10 melanoma cells (18). Within 1-2 weeks, this resulted in tumors of 1-2 mm diameter at the site of injection. M-3 melanoma tumors were similarly implanted in athymic nude mice by injection of approximately 10^6 M-3 melanoma cells (CCL-53.1 clone M-3, ATCC, Rockville, MD, USA), also resulting in tumors of 1-2 mm diameter within 1-2 weeks.

Laser treatment. Tumors were treated within 2 days of visual tumor detection. Mice were anesthetized *via* continuous inhalation using 2% Isofluorane (Baxter Healthcare Corporation, Deerfield, IL, USA) and placed on a heated bed to prevent hypothermia during treatment. Near infrared light from a Nd:YLF laser (DPM-1000, Coherent Scotland, Glasgow, UK) was passed through a two-element Galilean beam expander and then focused to a 50 μm waist using a planoconvex objective (0.05 N.A.). The axial position of the beam waist was made conjugate with the estimated center of the tumor, then delivered to the tumor and surrounding skin as a square, raster-scanned pattern (5 mm x 5 mm treatment area consisting of a 100 x 100 point array, 50 μs dwell time per point, 50 μm step size between points); the 1047 nm beam was rapidly and repeatedly scanned across the treatment area (ca. 1 s scan refresh rate) using a biaxial galvanometer system (model 6650, Cambridge Technology, Inc., Cambridge, MA, USA). Average power at the treatment site was 500 mW, with a delivered light dose of 1000 J/cm^2. Large tumors were treated by sequential treatment of adjacent areas until the entire apparent tumor area was completely treated with $2.5

mm margin on all sides with ca. 50% overlap of treatment areas. Following treatment, mice were observed for recovery from anesthesia. No evidence of pain or other discomfort was noted during or following laser treatment. Mice were then observed for a period of up to several months for evidence of tumor recurrence; those mice that exhibited recurrence were euthanized by CO_2 inhalation.

To allow elucidation of possible multiphoton and linear mechanisms in laser-tumor interaction, the Nd:YLF laser was operated in one of two modes: (1) mode-locked, yielding ca. 200 fs delivered pulse width at 120 MHz pulse repetition frequency; or (2) continuous wave, wherein cavity length was adjusted to preclude mode-locked pulse production. All other treatment parameters were identical, and mice were randomly assigned and treated with one of these operating modes.

Thermal imaging. An infrared camera (Thermacam PM-380, Inframetrics, North Billerica, MA, USA) and image capture software (ThermaGRAM 95, Thermoteknix, Cambridge, UK) was used to continuously observe surface thermal effects during laser treatment. This allowed estimation of mean and maximum surface temperature at the site of illumination.

Tissue preparation and spectroscopy. Freshly collected M-3 tumor tissue (ca. 25 mg) from an untreated mouse was rinsed with water, then placed into a 6-mL capped vial with 500 µL of Solvable (part no. 6NE9100, Packard Bioscience, Meriden, CT, USA). The contents of the vial were homogenized (PowerGen 125 Homogenizer, Fisher Scientific, Pittsburgh, PA, USA) for 5 s, and then centrifuged for 10 min. at approximately 1500 x g (model TJ-6 centrifuge, Beckman Coulter, Inc., Fullerton, CA, USA). After centrifugation, the resultant cell-free supernatant was diluted (ca. 100-fold) into a 1.5 mL methacrylate cuvette (Fisher Scientific), and its absorbance spectrum measured using a Genesys 2 UV-visible spectrometer (Thermo Spectronic, Inc., Rochester, NY, USA). An additional tissue specimen was homogenized in water and the resultant aqueous suspension diluted to obtain a spectrum illustrating melanin absorbance and tissue scatter.

Immunohistochemical assay. A cohort of laser treated mice (C57BL/6 mice with implanted B16-F10 tumors) were used to study immunologic response upon laser treatment. Samples of serum and tumor

tissue were analyzed for interferon-ã (IFN-ã), interleukin-2 (IL-2) and interlukin-10 (IL-10) using Cytoscreen™ test kits (BioSource International, Camarillo, CA, USA). Samples were collected immediately following laser treatment and at points 24-h and 72-h post-treatment; control samples were also collected at these time points from mice not receiving laser treatment.

Tumor challenge dose. One or more weeks after initial treatment, an additional cohort of laser treated mice (including both C57BL/6 and athymic nude mice previously receiving implantation of B16-F10 tumors) were injected in the opposite flank with a second dose of B16-F10 tumor cells (comprising 10^3 to 10^5 tumor cells). These mice were then observed for evidence of tumor retake (without further laser treatment) for a period of up to several months.

RESULTS

Gross and histologic response. Figure 1 illustrates a typical post-treatment progression for a B16-F10 tumor in an athymic nude mouse. Although a significant margin of normal skin was treated in the area surrounding the tumor, acute response is only noted at the site of the tumor, consisting of an area of obvious blanching with slight erythema. At 48-h post-treatment, a clearly demarcated eschar is evident that is confined to the tumor area. Within 1-2 weeks, the eschar exhibits signs of resolution, and upon full resolution (within 2-3 weeks) exhibits pigmented debris at the original tumor location. M-3 tumors were found to exhibit similar progression. No significant difference in gross outcome was noted for tumors treated with mode-locked laser radiation and those treated with continuous wave laser radiation, nor when comparing outcome in C57BL/6 and athymic nude mice.

Histologic response at 24-h post-treatment is illustrated in Figure 2, where part of a large M-3 tumor was treated, leaving a clearly demarcated border between treated (left-hand section of slide) and untreated (right-hand section) tumor tissue. The untreated section exhibits characteristic features of M-3 tumor cells: non-uniform pigmentation; marked pleomorphism; highly variable nuclei containing 2-6 nucleoli; multiple mitotic figures; and moderate vascularization. In contrast, the treated section exhibits

uniform, acute necrosis, with pyknotic nuclei, karyolysis and karyorrhexis; mild hemorrhage; and significant zones of pigmented cellular debris. Such histologic response is consistent with the gross response noted in Figure 1.

Thermal response. Surface thermal response during treatment of a B16-F10 tumor in an athymic nude mouse is illustrated in Figure 3. Thermograms show mean background temperature (i.e., "Mean Bkgnd") measured at an area of untreated normal skin near the tumor, mean temperature ("Mean") of each treatment area during treatment, and maximum temperature ("Max") observed within each treatment area. Note that the treatment regimen for this large tumor comprised sequential treatment of 25 adjacent treatment areas (i.e., as a 5 x 5 square array of individual treatment areas). Initial changes in temperature (above mean background temperature at 0-1200 s elapsed treatment time) illustrate that only small temperature increases occur as the laser is scanned across a region at the tumor margin that consists mostly of normal tissue. However, as the beam impinges upon areas consisting mostly or entirely of tumor tissue (i.e., at 1800-2400 s and 2800-3600 s), large increases in temperature are noted. Depending upon proximity of the subcutaneously-implanted tumor to the skin surface, some variation in the magnitude of mean and maximum response was noted (ca. ±5-10EC). It is also notable that mean and maximum temperature trended quickly to baseline once the treatment beam moved off of tumor tissue.

Outcome in athymic nude mice. Treatment outcome for various treatments and tumor models is summarized in Table 1; data correspond to number of treated tumors exhibiting complete response (i.e., no recurrence). While all animals exhibited comparable acute response (i.e., blanching followed by localized eschar formation), long-term response rate for the pigmented tumor (B16-F10) was markedly greater than for the amelanotic tumor (M-3). Furthermore, no significant difference in response rate was noted for treatment with mode-locked vs. continuous wave laser radiation.

Immunologic response. Tissue matched B16-F10 tumors implanted in C57BL/6 (i.e., immunocompetent) mice allowed assessment of immunologic response to laser treatment. Immunohistochemical assay results for serum and tumor tissue of laser-treated and untreated mice are

summarized in Tables 2 and 3. Three imunomodulators were examined: IL-2 (an immune system up-regulator); IFN-ã; and IL-10 (an immune system down-regulator). Serum levels were found to remain constant (within the limits of detection of the tests) for all test conditions. In contrast, intralesional levels were markedly affected at 24-72 hours post treatment: IFN-ã and IL-2 levels were elevated at 24 hours, and IL-10 was elevated by 72 hours. These findings indicate that laser treatment produces a significant, localized immune response.

Tumor challenge data allows the significance of the immunohistochemical data of Tables 2 and 3 to be assessed, and is summarized in Table 4. The observed tumor take rate for various challenge doses illustrates that once the initial tumor has been destroyed it cannot be re-established in immunocompetent mice (i.e., C57BL/6); in contrast, immune-deficient mice (i.e., athymic nudes) exhibit no such immune response following laser treatment.

DISCUSSION

Both M-3 (amelanotic) and B16-F10 (normally pigmented) tumor models were studied in an effort to elucidate the relevance of potential non-linear and linear photoactivation mechanisms. M-3 tumors produce normal levels of eumelanin and pheomelanin precursors, but are deficient in means to polymerize these precursors into melanin. Thus, the M-3 model provides a sensitive test for non-linear photoactivation, since the potentially phototoxic precursors are present (and capable of undergoing two- or three-photon excitation to a phototoxic state) while melanin levels (and hence potential for linear, hyperthermic effects upon linear absorbance of applied laser energy) are minimal. While the data in Table 1 show a greater response rate for laser activation of M-3 tumors using mode-locked radiation, these differences do not appear to be statistically significant. Furthermore, no acute gross or histologic differences were noted upon comparison of treatments under these two laser modes. Moreover, the results for B16-F10 tumors are markedly better, while again exhibiting no significant difference in clinical outcome, nor in acute gross or histologic outcome. Taken together, these results imply that thermal effects are the predominant mechanism

in tumor destruction.

The thermal data illustrated in Figure 2 shows that mean tumor temperature is increased into the 45-55EC temperature range during laser treatment, and that this increased temperature is maintained for >100 s. Niemz (19) shows that such combination of elevated temperature and duration yields irreversible hyperthermia, which is consistent with histologic observations of this study (i.e., tissue necrosis). The maximum temperature appears to be much higher at the focus of the beam (i.e., $60EC), which, according to Niemz, is consistent with coagulation and possible denaturation. However, this highly elevated temperature is only experienced in a given volume of tumor tissue while the rapidly rastered focus is directed into that volume (i.e., high-speed measurements of tissue temperature illustrate that the maximum temperature only occurs in a give volume for 1 ms or less, and that this high-temperature zone tracks the motion of the beam across the tumor). Thus, it appears that a rapid spike in temperature (i.e., from the elevated average temperature to a maximum temperature then back to the average) may contribute to cellular photodisruption without wholesale denaturation of tumor proteins and other potentially antigenic materials. Such effects appear to be evidenced by acute tissue blanching (which becomes clearly evident within the first 10-20 s of laser treatment) as well as acute necrosis noted upon histologic examination.

Impulse heating, combined with sustained hyperthermic conditions, yields massive, acute coagulative necrosis of treated lesions yet appears to avoid complete destruction of antigenic materials present in or on destroyed cells; such destruction of antigens would occur upon sustained heating to temperatures in excess of 60EC, for example as occurs in laser-induced interstitial thermotherapy. In contrast, the present treatment regimen appears to yield localized, rapid release (i.e., unmasking) of large quantities of intact antigenic materials from the treated lesions. Although no systemic immune response is evident (as illustrated by the serum data in Table 2, as well as lack of any other observable systemic effects, such as lethargy, fever, or edema proximal to the treated lesion), a potent localized response occurs within 24-h post-treatment (as evidenced by markedly increased levels of IFN-ã and IL-2 shown in Table 3). Presence of pro-inflammatory cytokines (i.e., IL-2) at 24-h, followed by appearance of anti-

inflammatory cytokines (IL-10) within 72-h, is consistent with an acute, localized immune-system insult that begins to undergo resolution within this time frame. Contemporaneous formation of a localized eschar supports the assertion that the initial immune response is rapid, potent, and highly localized.

The relevance of this immune response is dramatically manifest by the tumor challenge data of Table 4. Here, immunocompetent mice (i.e., C57BL/6) prove capable of rejecting massive challenge doses once they have received laser treatment of a primary lesion. In contrast, laser-treated immune-deficient mice (athymic nudes) are incapable of rejecting such challenge doses. The data in Table 4 suggest that onset of this anti-tumor immunity is rapid (within 1 week post-treatment) and permanent.

Efforts to demonstrate spontaneous remission of an untreated secondary tumor upon treatment of a similar contra-lateral primary tumor proved untenable, however, because the tumor models used in this study yield extremely virulent tumors characterized by massive, exponential rates of growth once they have reached detectable size. Such secondary tumors thus become far too large for the murine immune system to control by the time any anti-tumor immune response has developed. Fortunately, such tumor models do not accurately mimic the majority of human tumors, which exhibit relatively slow growth rates. Thus, it appears possible that laser treatment of a primary human tumor could lead to immunologic destruction of microscopic metastatic tumors or clusters of tumor cells. Indeed, *any* success in controlling these virulent murine tumors augurs well for potential efficacy in humans, where slower tumor growth rates and the presence of an intact immune system should aid in eradicating any residual tumor cells not directly destroyed by the laser treatment.

It is also notable that the reported results comprise successful treatment of such virulent tumors with thicknesses of 3 mm and greater. The laser wavelength used in this work was selected to facilitate delivery of sufficient therapeutic light to the base of such relatively thick tumors. The spectra in Figure 4 illustrate that melanin exhibits significant optical cross section well into the NIR, while the only other significant chromophor at such wavelengths (i.e., water, which is the only potential alternate chromophor of sufficient concentration within tumors to be relevant; spectral data shown adapted from ref. 20) exhibits

insignificant potential for interference in the NIR. Although previous studies have suggested that ca. 810 nm is optimal for delivery of light into melanoma tissue (10, 11), this appears to be based on erroneous interpretation of reported water absorption at longer wavelengths. Since the cross section for melanin at 810 nm is approximately 3x that of 1047 nm, it is likely that a commensurate difference in light penetration depth exists between these two wavelengths. Markedly reduced efficacy for treatment of retinal tumors $3 mm thick using 810 nm light (10, 11), compared with excellent results of the present study for treatment of tumors of such thickness, suggests that use of light at ca. 1000-1100 nm facilitates delivery of sufficient applied energy throughout the full thickness of the tumor, while continuing to afford adequate, selective absorption of applied energy within melanotic tissues. Lack of side effects in laser-treated normal skin suggests that such NIR light also affords superior safety, since no significant secondary absorbers of such applied light exist in skin or underlying tissues.

Finally, comprehensive studies by Krause et al. (21) using the Nd:YLF laser to treat B16-F10 tumors implanted in the choroid of immune-suppressed rabbits corroborate the remarkable efficacy of this treatment regimen, and support the present authors' hypotheses concerning hyperthermic and photodisruptive mechanisms. In Krause's work, a single treatment of $125 J/cm^2 led to >90% eradication of retinal tumors with a mean thickness of ca. 3 mm. Both gross and histologic outcomes were identical to those reported here for cutaneous tumors.

CONCLUSIONS

Treatment of cutaneous melanoma with rapidly-scanned, tightly-focused NIR light appears to elicit selective hyperthermic and photodisruptive destruction of tumor tissue. Potential non-linear effects due to multiphoton excitation of melanin precursors appear to be of minimal significance. Since the effects are localized to the treated lesion, suppression of the host's immune system (such as is associated with conventional radiation therapy and chemotherapy) is avoided, enabling the host to achieve maximal immune response to released tumor antigens and residual tumor tissues. Accordingly, such treatment is capable of stimulating an acute, localized inflammatory response leading to long-lasting systemic anti-tumor immunity. Stimulation of such immunity may, in humans, lead to improved outcome at both the treatment site and at sites of distant metastasis.

REFERENCES

1. Cancer facts & figures 2001 (2001) American Cancer Society.

2. Dougherty, T.J., C.J. Gomer, B.W. Henderson, G. Jori, D. Kessel, M. Korbelik, J. Moan, and Q. Peng (1998) Photodynamic therapy. *J. Natl. Cancer Inst.* **90**, 889-905.

3. Busetti A, M. Soncin, G. Jori, M.E. Kenney, and M.A. Rodgers (1998) Treatment of malignant melanoma by high-peak-power 1064 nm irradiation followed by photodynamic therapy. *Photochem Photobiol*. **68**, 377-381.

4. S. Schmitz, P.D. Thomas, T.M. Allen, M.J. Poznansky and K. Jimbow (1995) Dual role of melanins and melanin precursors as photoprotective and phototoxic agents: inhibition of ultraviolet radiation-induced lipid peroxidation. *Photochem. Photobiol*. **61**, 650-655.

5. Rogers, R.S. 3rd and L.E. Gibson (1997) Mucosal, genital, and unusual clinical variants of melanoma. *Mayo Clin. Proc.* **72**, 362-366.

6. Riley, P.A. (1997) Melanin. *Int. J. Biochem. Cell Biol.* **29**, 1235-1239.

7. Fisher, W.G., W.P. Partridge, C. Dees and E.A. Wachter (1997) Simultaneous two-photon activation of type-I photodynamic therapy agents. *Photochem. Photobiol*. **66**, 141-155.

8. Wachter, E.A., M.G. Petersen, and H.C. Dees (1999) Photodynamic therapy with ultrafast lasers. In: Reed, M.K., and J. Neev, editors. Commercial and biomedical applications of ultrafast lasers; *SPIE Proceedings* **3616**, 66-74.

9. Anderson, R.R. and J.A. Parrish (1981) The optics of human skin. *J. Invest. Derm*. **77**, 13-19.

10. Oosterhuis, J.A., H.G. Journée-de Korver, H.M. Kakebeeke-Kemme, and J.C. Bleeker (1995) Transpupillary thermotherapy in choroidal melanomas. *Arch. Ophthalmol*. **113**, 315-321.

11. Shields, C.L., J.A. Shields, J. Cater, N. Lois, C. Edelstein, K. Gündüz, and G. Mercado (1998) Transpupillary thermotherapy for choroidal melanoma. *Ophthalmol.* **105**, 581-590.

12. Korbelik, M., G. Krosl, J. Krosl, and G.J. Dougherty (1996) The role of host lymphoid populations in the response of mouse EMT6 tumor to photodynamic therapy. *Cancer Res.* **56**,

5647-5652.

13. Korbelik, M. (1996) Induction of tumor immunity by photodynamic therapy. *J. Clin. Laser Med. Surg.* **14**, 329-334.

14. Krosl, G., M. Korbelik, J. Krosl, and G.J. Dougherty (1996) Potentiation of photodynamic therapy-elicited antitumor response by localized treatment with granulocyte-macrophage colony-stimulating factor. *Cancer Res.* **56,** 3281-3286.

15. Gollnick, S.O., X. Liu, B. Owczarczak, D.A. Musser, and B.W. Henderson (1997) Altered expression of Interleukin 6 and Interleukin 10 as a result of photodynamic therapy in vivo. *Can. Res.* **57**, 3904-3909.

16. Korbelik, M. and I. Cecic (1999) Contribution of myeloid and lymphoid host cells to the curative outcome of mouse sarcoma treatment by photodynamic therapy. *Cancer Lett.* **137**, 91-98.

17. Korbelik, M. and G.J. Dougherty (1999) Photodynamic Therapy-mediate immune response against subcutaneous mouse tumors. *Cancer Res.* **59,** 1941-1946.

18. B16-F10 melanoma cells were a kind gift of Dr. Lucy Young, Massachusetts Eye and Ear Infirmary, Boston, MA, USA.

19. Niemz, M.H. (1996) *Laser-Tissue Interactions, Fundamental and Applications*, pp. 77-80. Springer, Berlin.

20. van den Berg, T.J.T.P. and H. Spekreijse (1997) Near infrared light absorption in the human eye media. *Vision Res*. **37**, 249-253.

21. Matthias Krause, M., J. Xiong, E.S. Gragoudas, and L.H.Y. Young, Treatment of experimental choroidal melanoma with a neodymium:yttrium lanthanum fluoride laser at 1047 nm. *Arch. Ophthalmol*. (in press).

Table 1. Treatment outcome, as defined by complete response (i.e., no recurrence) of treated tumor. *cw* indicates continuous wave laser radiation. Average tumor thickness < 3 mm.

Tumor	Mouse	Laser mode	
		mode-locked	*cw*
M-3	nude	3 / 8	1 / 7
B16-F10	nude	10 / 12	9 / 9

Table 2. Comparison of serum immunomodulator levels for untreated and laser-treated C57BL/6 mice having implanted B16-F10 tumors. Latency period following treatment is as indicated. There were no statistically significant differences in serum immunomodulator expression (assessed *via* two-way ANOVA) within treatment groups or between treatment groups.

Immunomodulator	Treatment	Serum Level (pg / mL)		
		0 h	24 h	72 h
IFN-ã	Untreated	407 ± 11	416 ± 18	414 ± 11
	Laser Treated	417 ± 15	415 ± 18	416 ± 8
IL-2	Untreated	221 ± 17	210 ± 26	238 ± 36
	Laser Treated	217 ± 75	252 ± 18	231 ± 27

Table 3. Comparison of intralesional immunomodulator levels. Statistically significant differences (assessed *via* two-way ANOVA) are detectable for the laser-treated groups (at 24 and 72 h for IFN-ã and IL-2 and at 72 h for IL-10).

Immunomodulator	Treatment	Serum Level (pg / µg protein)		
		0 h	24 h	72 h
IFN-ã	Untreated	93 ± 17	117 ± 45	87 ± 29
	MPE Treated	93 ± 17	290 ± 51	320 ± 30
IL-2	Untreated	127 ± 19	156 ± 24	143 ± 47
	MPE Treated	105 ± 34	258 ± 23	264 ± 19
IL-10	Untreated	53 ± 12	47 ± 18	57 ± 9
	MPE Treated	57 ± 16	64 ± 16	230 ± 41

Table 4. Outcome of tumor challenge dose (i.e., tumor take rate) at various intervals following laser treatment of B16-F10 tumor. Implantation rate for naive mice illustrates that, in the absence of an anti-tumor immune response, > 90% tumor take rate is expected upon implantation of 10^4 tumor cells.

Implantation	Challenge	B16-F10 Dose	Tumor Take	
		(cells)	C57BL/6	Athymic Nude
Naive	-	10^4	28 / 30	-
Laser treated	1 week post-treatment	10^3 - 10^5	0 / 6	6 / 6
Laser treated	2 weeks post-treatment	10^3 - 10^4	0 / 8	-
Laser treated	3-4 months post-treatment	10^5	0 / 5	-

FIGURE CAPTIONS

Figure 1. Typical progression for B16-F10 tumor in athymic nude mouse following laser treatment.

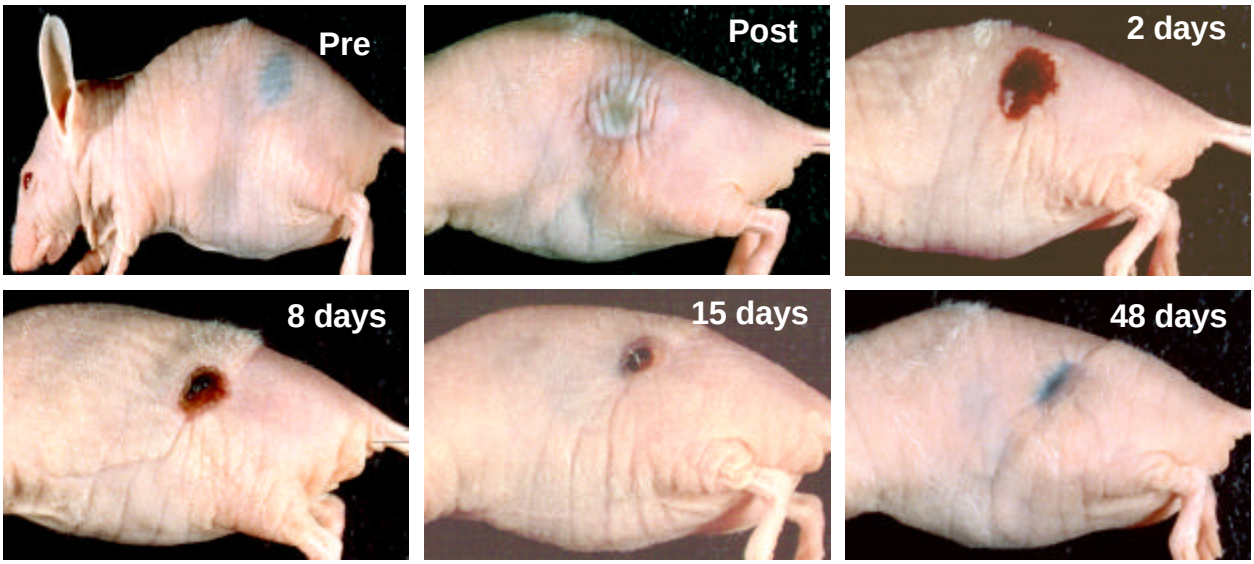

Figure 2. Tissue section, H&E stained, from M-3 tumor implanted in athymic nude mouse (100x magnification). Left-hand section of tumor laser treated, right-hand section untreated.

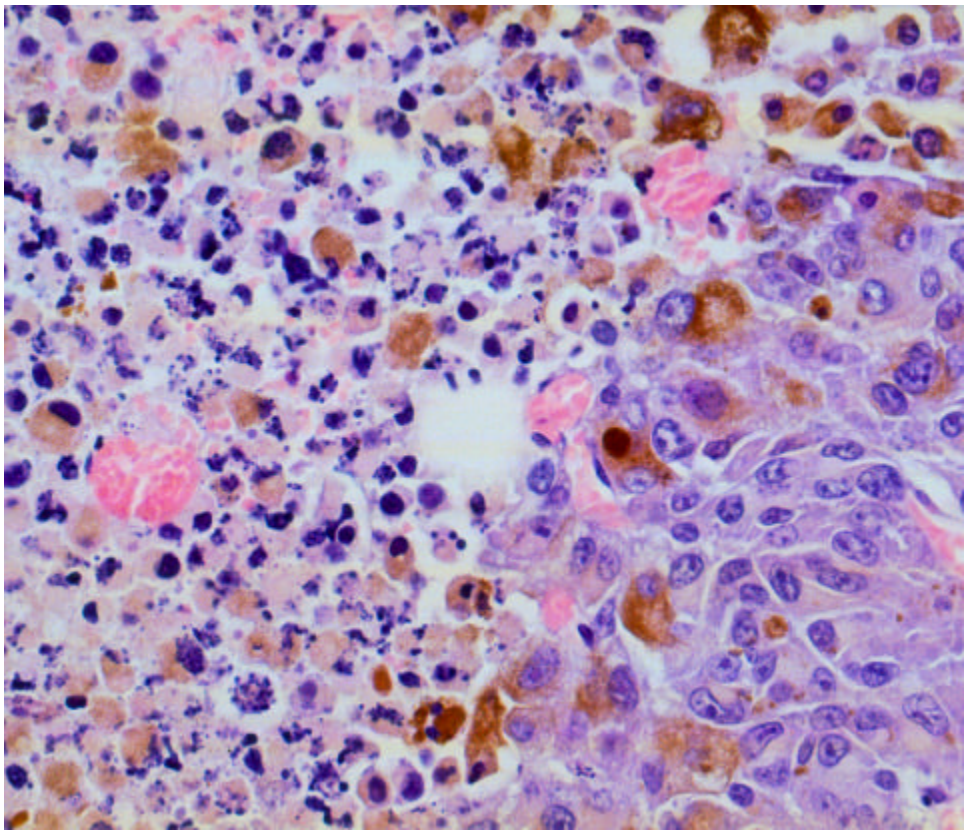

Figure 3. Surface thermal response of B16-F10 tumor during laser treatment. Thermograms illustrate mean background temperature (i.e., “Mean Bkgnd”) of untreated normal skin, mean temperature (“Mean”) of treatment area during treatment, and maximum temperature (“Max”, shown by dashed line) within treatment area.

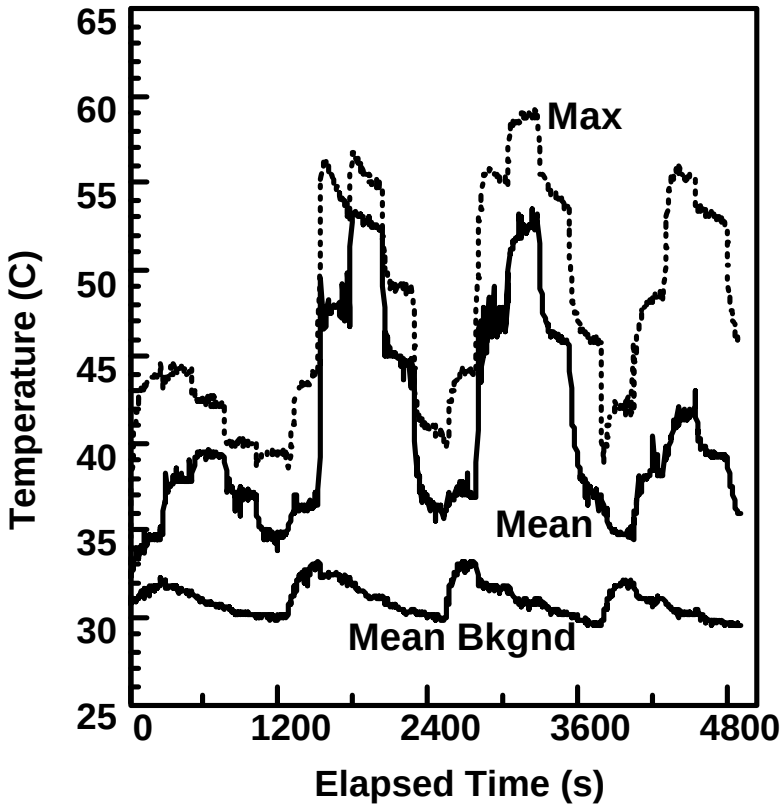

Figure 4. Comparison of absorbance spectra of diluted M-3 tumor cell suspension and cell extract, lysed whole blood, and water (20). Dashed line illustrates treatment wavelength. Optical density of biological materials is not corrected for dilution.